Electronic Supplementary Material (ESI) for Journal of Materials Chemistry A.
This journal is © The Royal Society of Chemistry 2022

**Supporting Information**

# High-energy Conversion-type Cathode Activated by Amorpholization for Li Rechargeable Batteries

*YongSeok Lee[a,b], Jungmin Kang[a,b], Jinho Ahn[a,b], Wonseok Ko[a,b], Hyunyoung Park[a,b], Seokjin Lee[a,b], Sangyeop Lee[a,b], Jung-Keun Yoo[c,*] and Jongsoon Kim[a,b,*]*

[a]Department of Energy Science, Sungkyunkwan University, Suwon, 16419, Republic of Korea

[b]SKKU Institute of Energy Science and Technology (SIEST), Sungkyunkwan University, Suwon 16419, Republic of Korea

[c]Carbon Composites Department, Composites Research Division, Korea Institute of Materials Science (KIMS), 797 Changwondaero, Changwon, Republic of Korea

Corresponding Authors: Dr. Jung-Keun Yoo (E-mail: yoojk@kims.re.kr), Prof. Jongsoon Kim (E-mail: jongsoonkim@skku.edu)

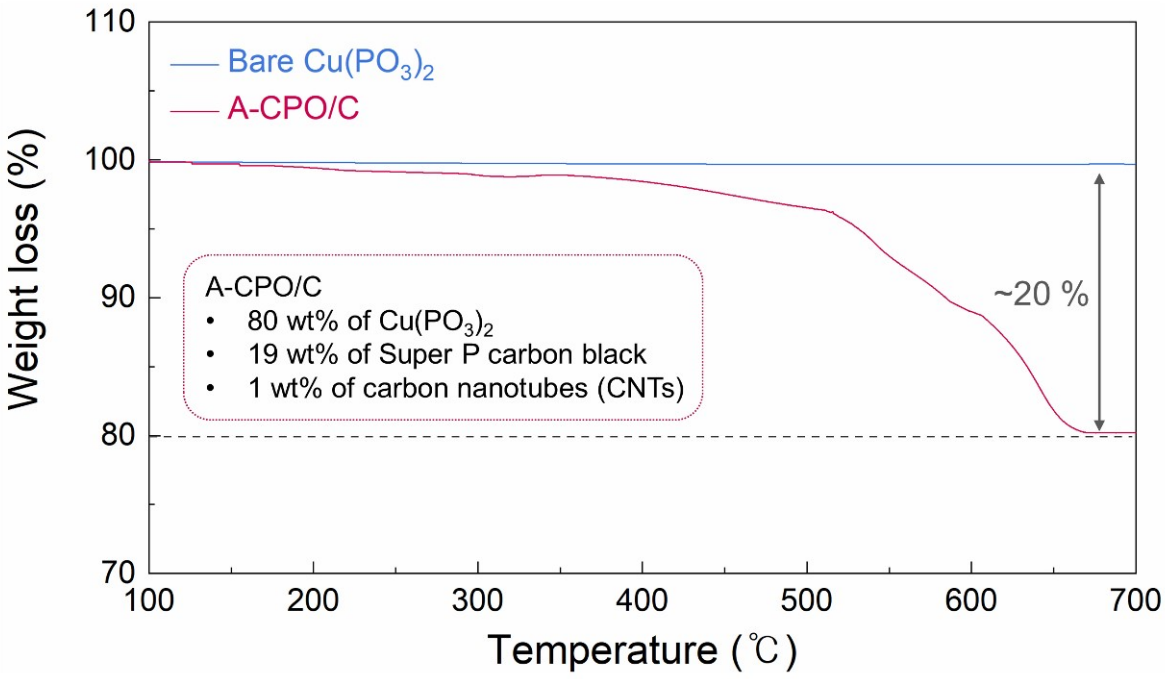


**Fig. S1** Thermogravimetric (TGA) spectra profiles of bare $Cu(PO_3)_2$ and A-CPO/C.

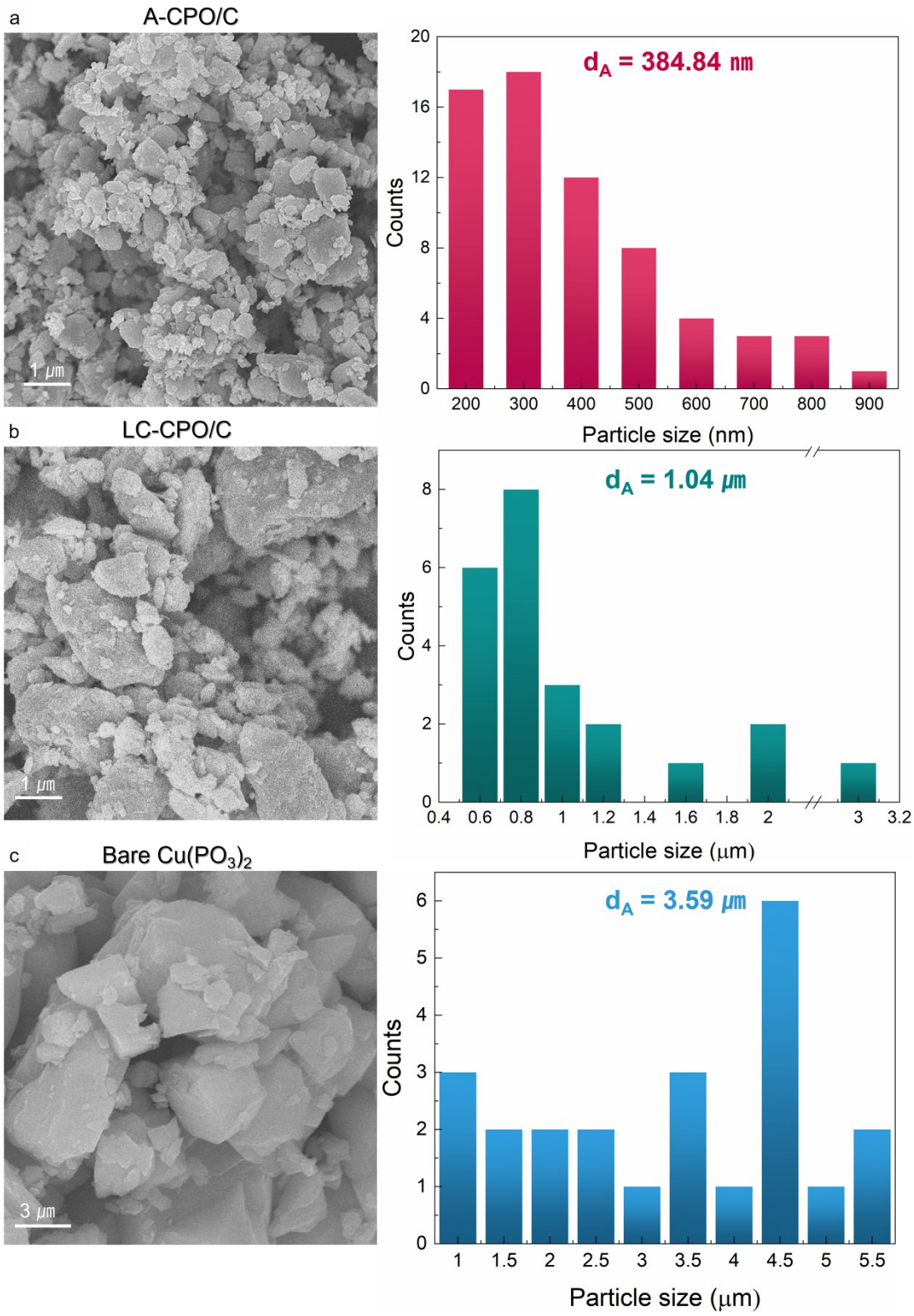


**Fig. S2** Comparing SEM images and average particle sizes of (a) A-CPO/C, (b) LC-CPO/C, (c) bare $Cu(PO_3)_2$.

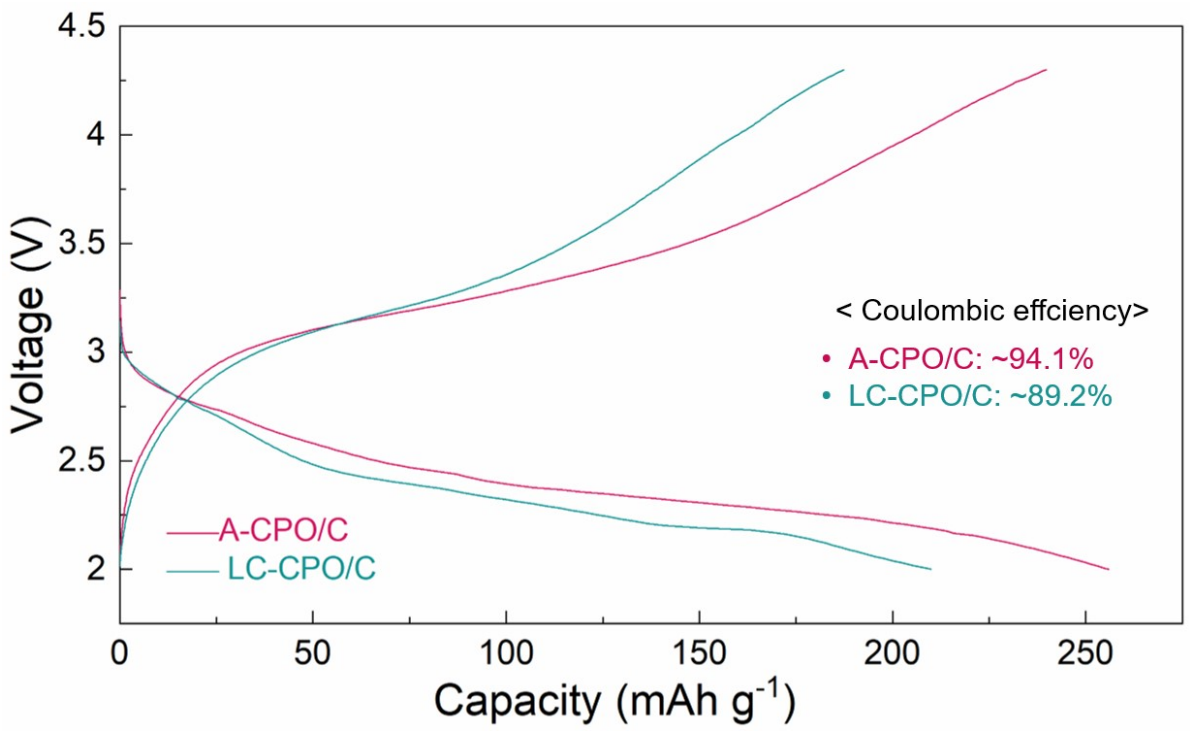


**Fig. S3** Comparing charge/discharge curves for pre-cycle at 12 mA $g^{-1}$ of A-CPO/C and LC-CPO/C.

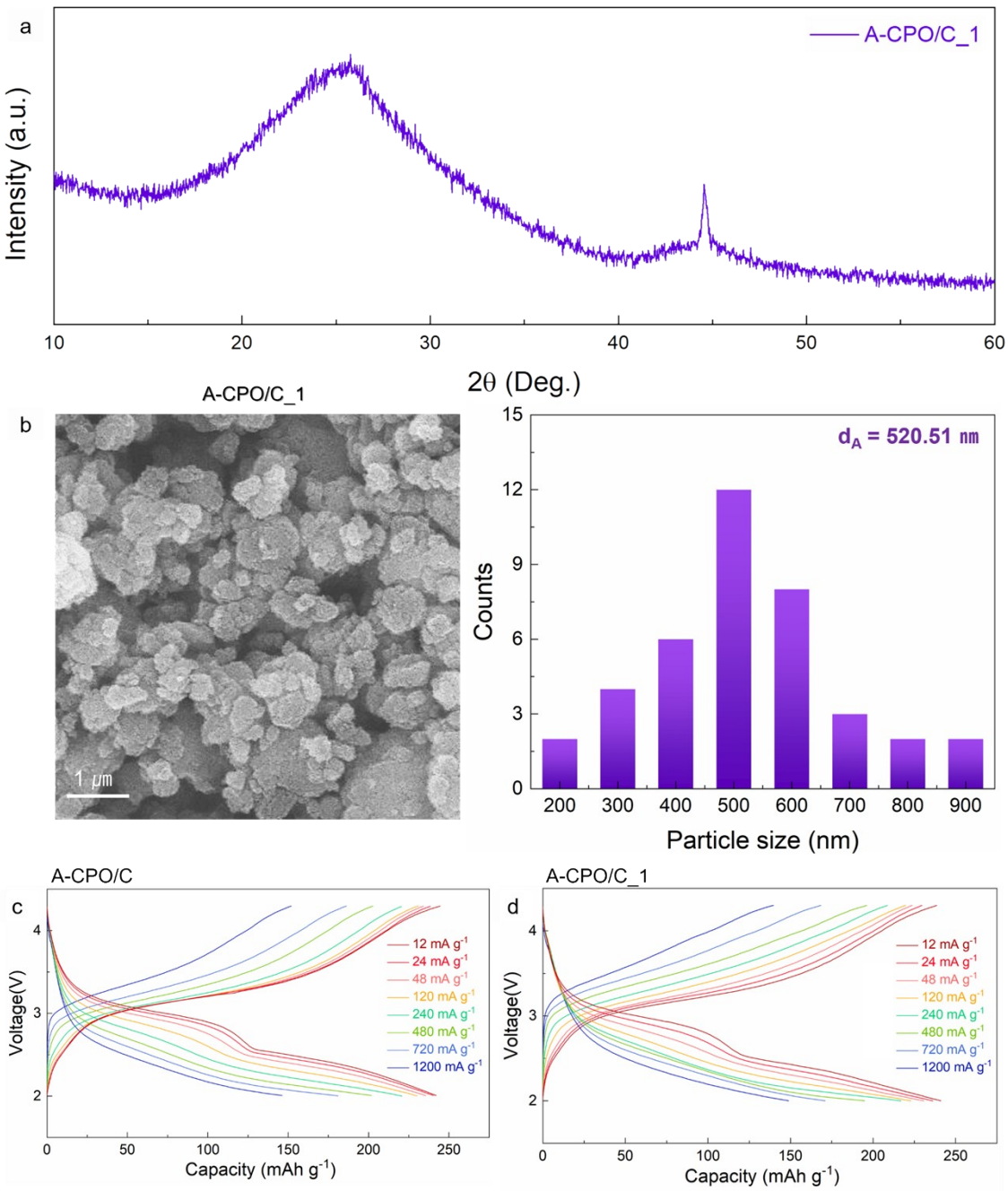


**Fig. S4** (a) XRD pattern, (b) SEM image and average particle size of A-CPO/C_1. (c) Comparing power capability performances of samples for (c) A-CPO/C, (d) A-CPO/C_1. [Preparation process of A-CPO/C_1: After preparation of the amorphorized $Cu(PO_3)_2$ without conductive carbons through the ball-milling process at 550 rpm for 10 h at first, the amorphorized $Cu(PO_3)_2$ was mixed with conductive carbons through the ball-milling process at 400 rpm for 12 h]

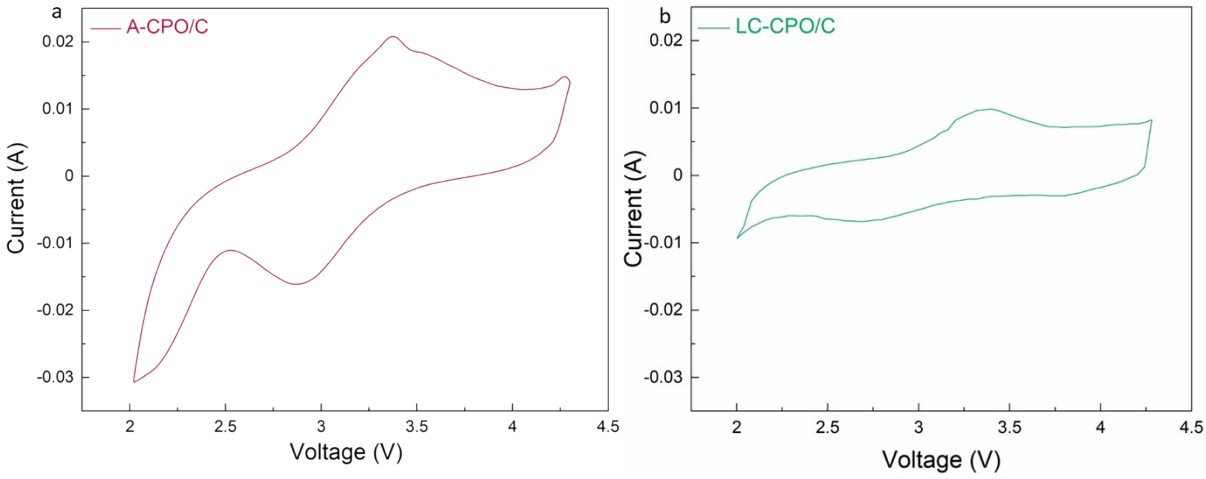


**Fig. S5** Comparing CV curves of (a) A-CPO/C, (b) LC-CPO/C electrode measured at 5 mV $s^{-1}$ in the voltage range of 2.0–4.3 V (*vs.* $Li^+/Li$)

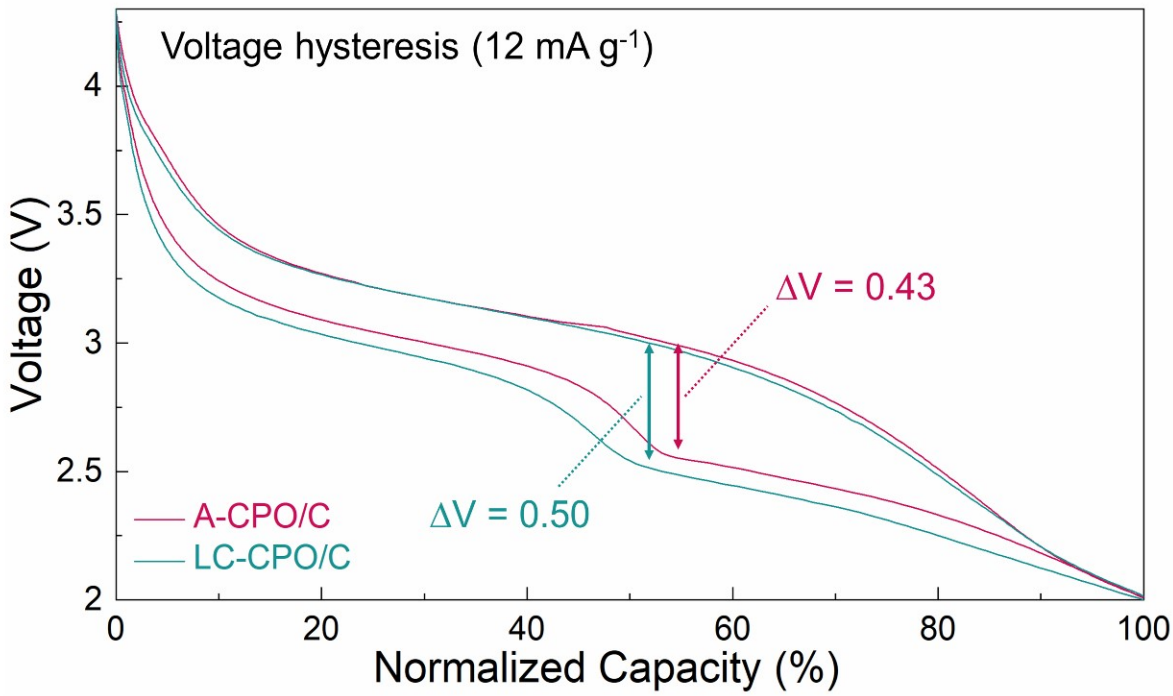


**Fig. S6** Comparison charge/discharge hysteresis of A-CPO/C and LC-CPO/C electrodes measured at 12 mA $g^{-1}$.

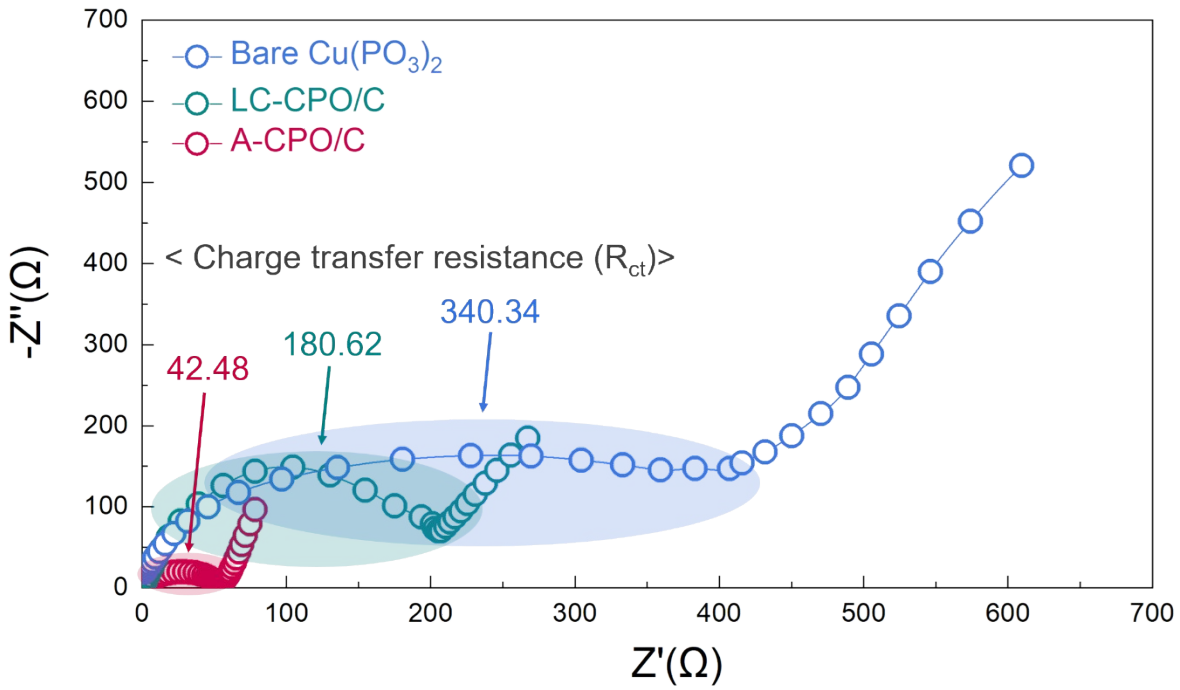


**Fig. S7** EIS measurements and values of charge transfer resistance of bare $Cu(PO_3)_2$, LC-CPO/C and A-CPO/C

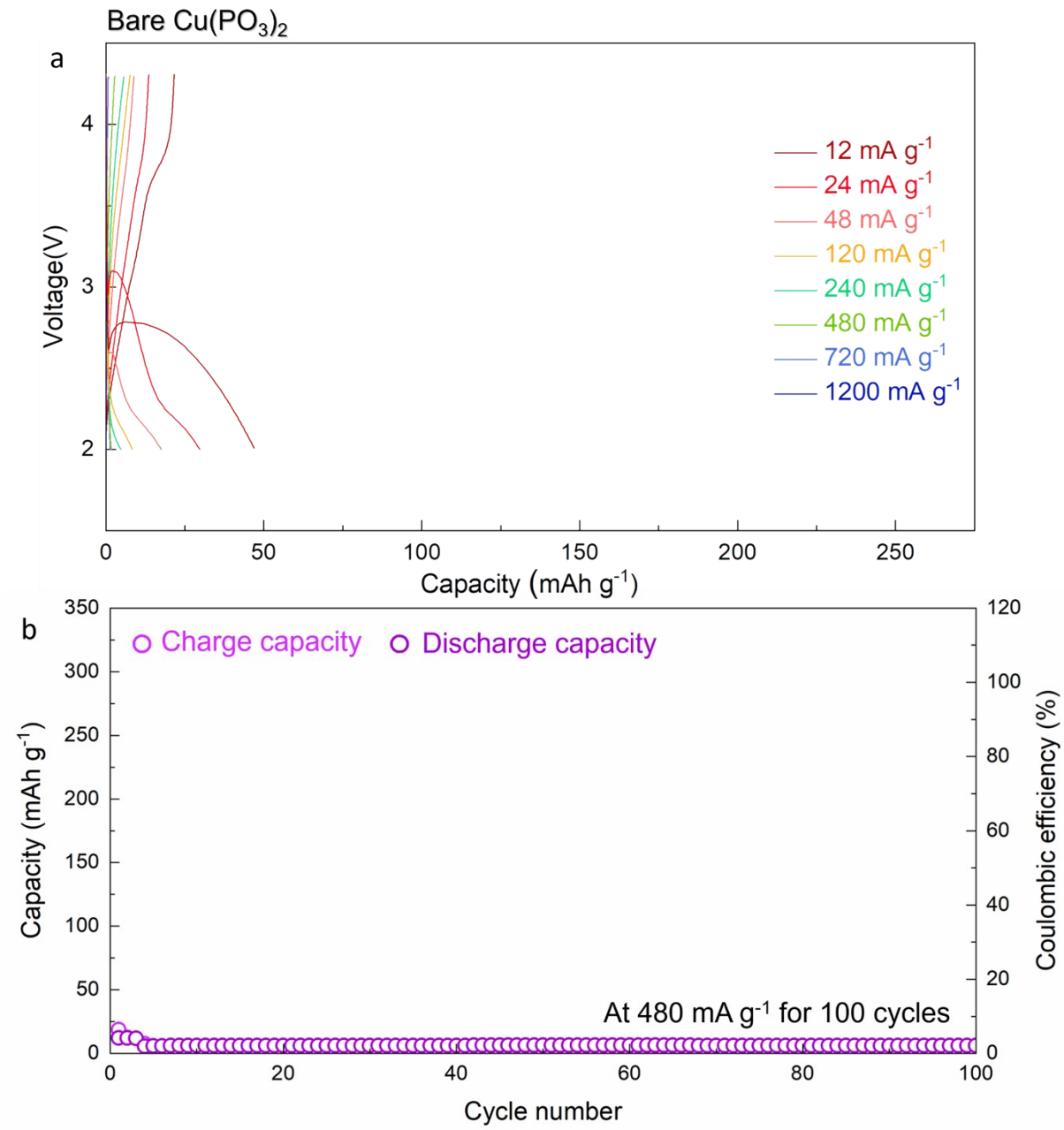


**Fig. S8** (a) Power capability at various current density, (b) cycle performance for 100 cycles at 480 mA $g^{-1}$ of bare $Cu(PO_3)_2$.

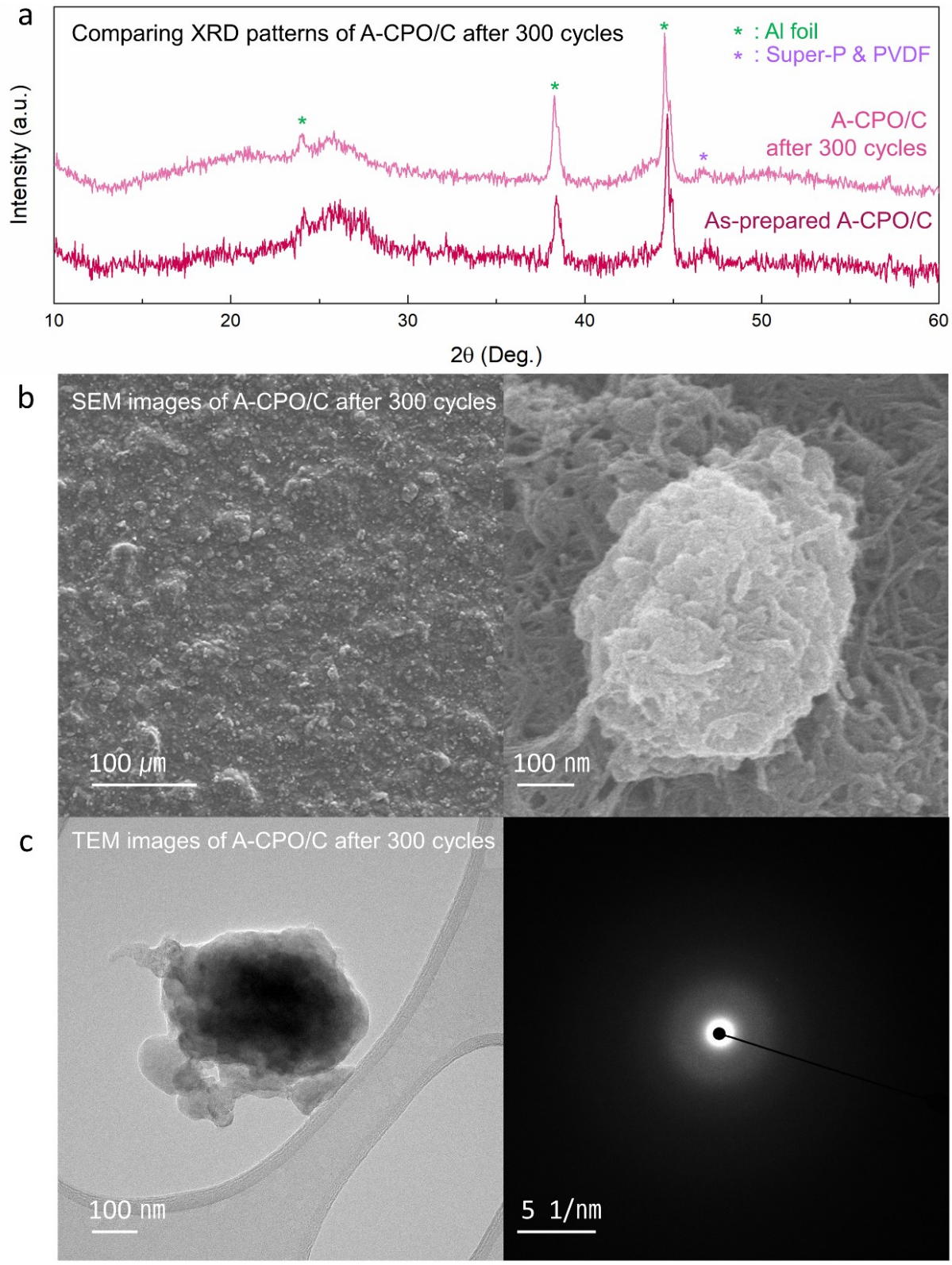


**Fig. S9** Comparing (a) XRD patterns, (b) SEM image, (c) TEM image and SAED pattern of both of as-prepared/after 300cycles for A-CPO/C electrode

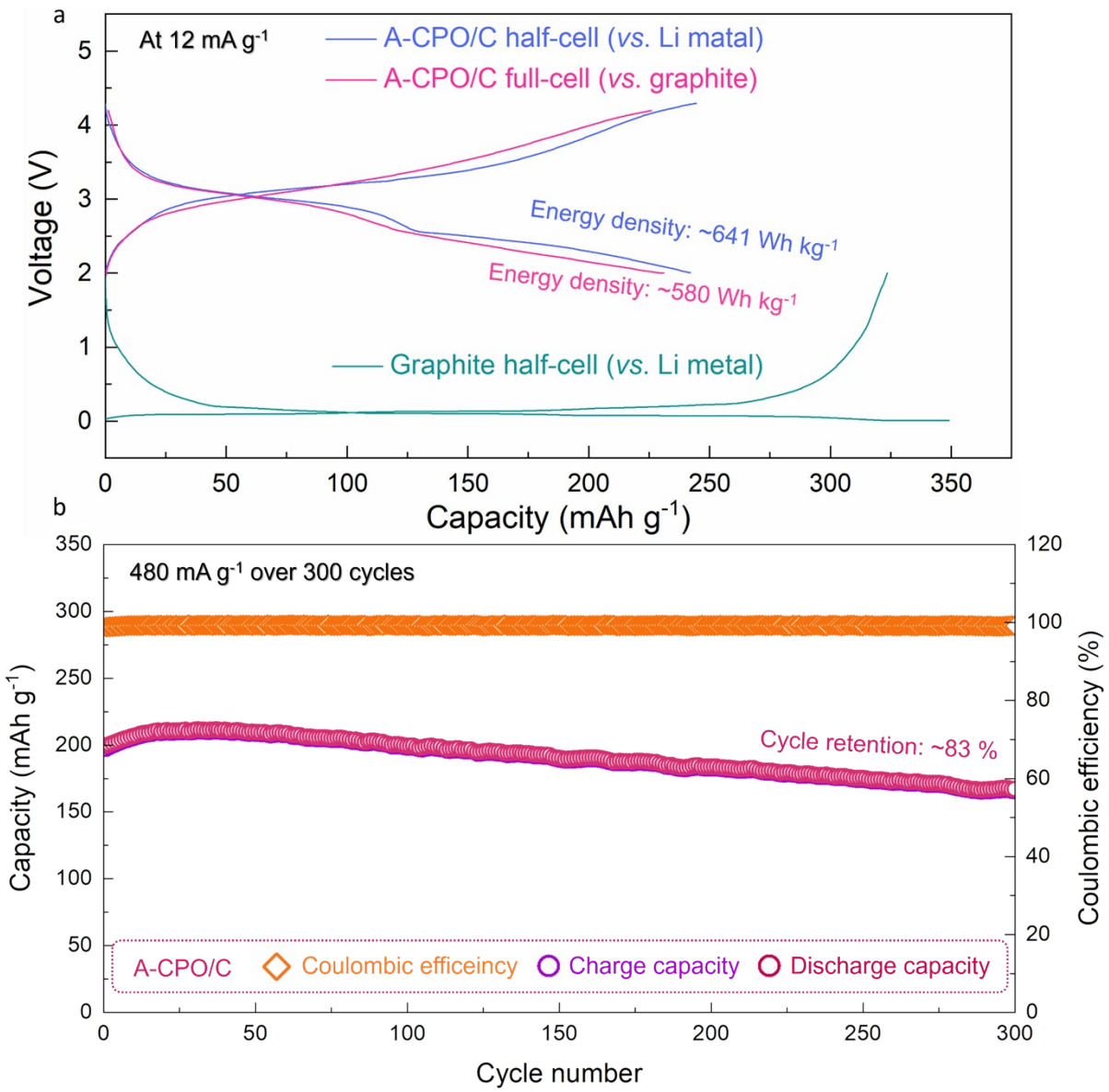


**Fig. S10** (a) Charge/discharge curves of A-CPO/C half-cell (*vs*. Li metal), full-cell (*vs*. graphite) and graphite half-cell (*vs*. Li metal) at 12 mA $g^{-1}$, (b) Cycle performance of A-CPO/C full-cell for 300 cycles at current density of 480 mA $g^{-1}$.

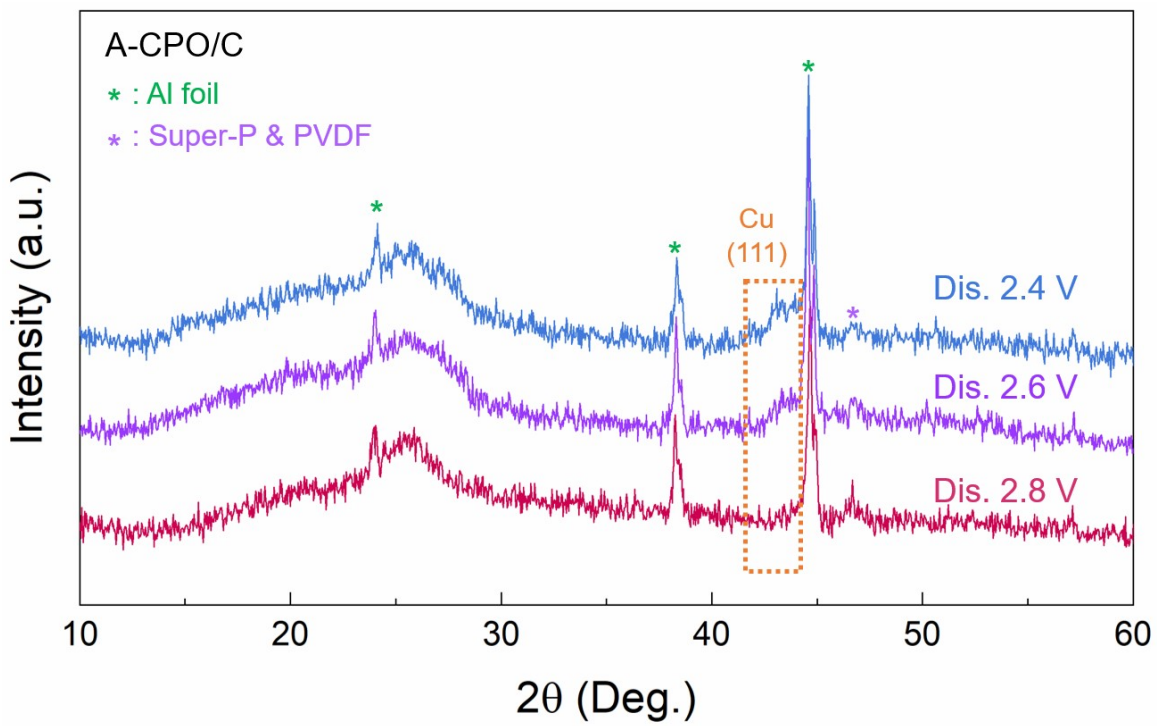


**Fig. S11** *Ex-situ* XRD patterns of discharged A-CPO/C electrodes at 2.4, 2.6 and 2.8 V

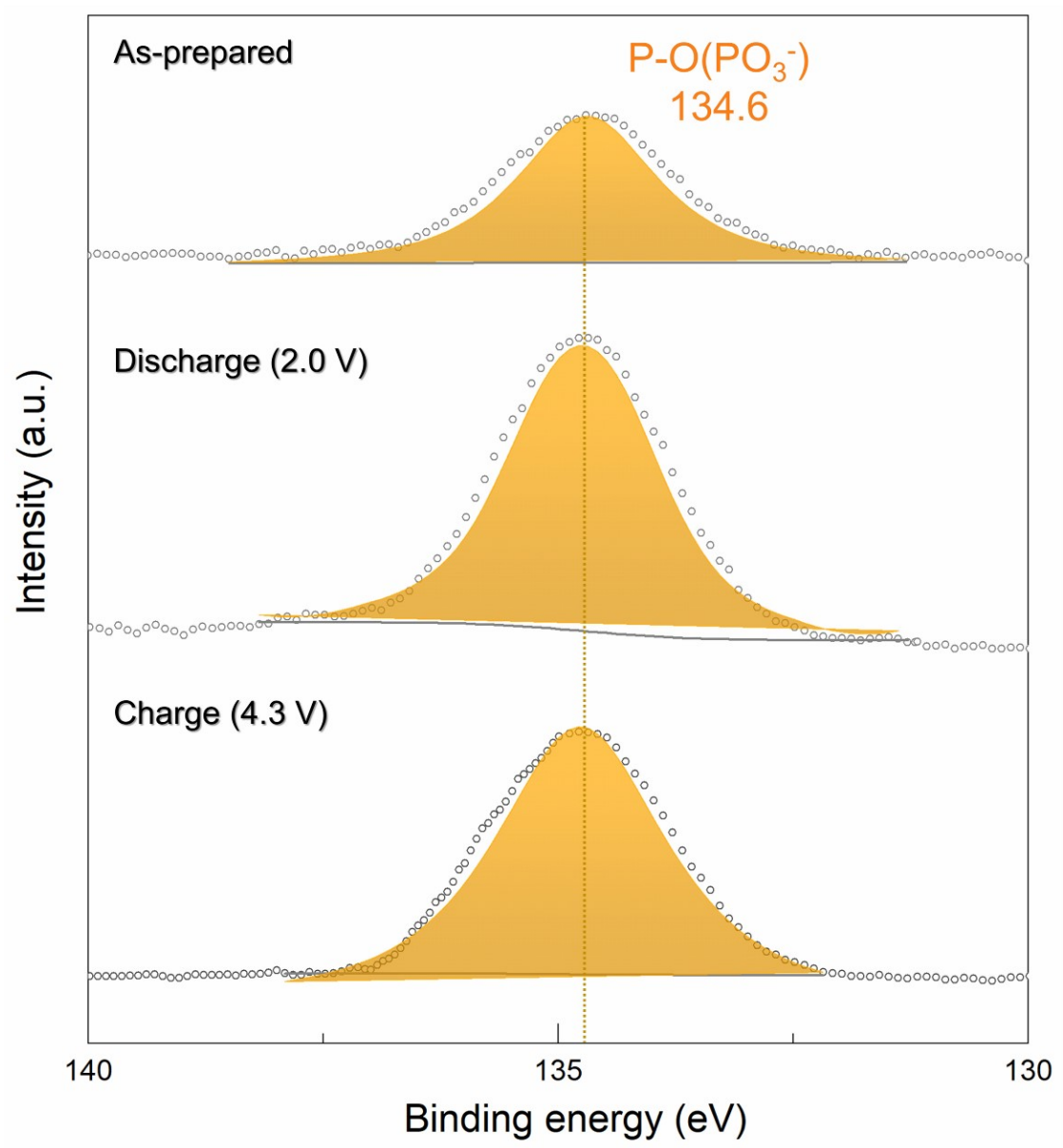


**Fig. S12** *Ex-situ* measurements of as-prepared, discharged and charged A-CPO/C electrodes for XPS P 2p spectra.

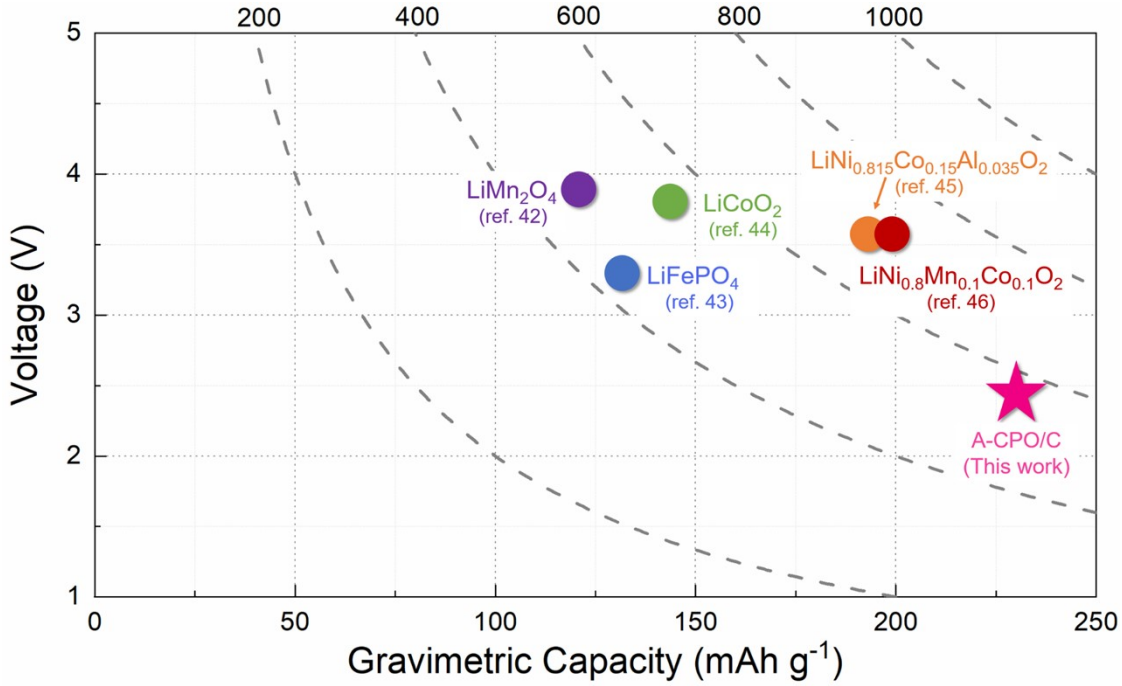


**Fig. S13** Comparison of energy densities (based on weights of active cathode materials) A-CPO/C and the other conventional cathodes in full-cell system

**Table S1** ICP analyses on the atomic ratio of Cu, P and O of $Cu(PO_3)_2$.

| Material | Cu | P | O |
|---|---|---|---|
| $Cu(PO_3)_2$ | 1.004 | 1.997 | 6.012 |

**Table S2** Formation energies of $Cu(PO_3)_2$, $Li(PO_3)$, Cu and Li and predicted theoretical redox potentials of (a) $Cu(PO_3)_2$, (b) CuO using first principles calculation

a

| $Cu(PO_3)_2$(*vs.* $Li^+/Li$): $Cu(PO_3)_2 + 2Li^+ + 2e^- \leftrightarrow Cu + 2LiPO_3$ | |
|---|---|
| Compound | Formation E (eV/f.u.) |
| $Cu(PO_3)_2$ | -60.4305 |
| Li | -1.8911 |
| Cu | -3.7538 |
| $LiPO_3$ | -33.6555 |
| Theoretical voltage of $Cu(PO_3)_2$ : -3.4260 (*vs.* $Li^+/Li$) | |

b

| CuO(*vs.* $Li^+/Li$): $CuO + 2Li^+ + 2e^- \leftrightarrow Cu + Li_2O$ | |
|---|---|
| Compound | Formation E (eV/f.u.) |
| CuO | -10.2458 |
| Li | -1.8911 |
| Cu | -3.7538 |
| $Li_2O$ | -14.0091 |
| Theoretical voltage of CuO : -1.8674 (*vs.* $Li^+/Li$) | |